[6]B. Domeij, F. Brown, J. A. Davies, and M. McCargo, Can. J. Phys. 42, 1624 (1964).
[7]J. A. Davies, Atomic Energy of Canada, Ltd., Report No. AECL-2757, 1967 (unpublished).
[8]E. V. Kornelsen, F. Brown, J. A. Davies, B. Domeij, and G. R. Piercy, Phys. Rev. 136, A849 (1964).
[9]F. Brown, G. C. Ball, D. A. Channing, L. M. Howe, J. P. S. Pringle, and J. L. Whitton, Nucl. Instr. Methods 38, 249 (1965).
[10]D. Powers, W. K. Chu, and P. D. Bourland, Phys. Rev. 165, 376 (1968); W. K. Chu, P. D. Bourland, K. H. Wang, and D. Powers, *ibid.* 175, 342 (1968).
[11]R. J. MacDonald and D. Haneman, J. Appl. Phys. 37, 3048 (1966).
[12]F. Brown and J. A. Davies, Can. J. Phys. 41, 844 (1963).
[13]L. B. Magnusson, Phys. Rev. 81, 285 (1951).
[14]S. Yosim and T. H. Davies, J. Phys. Chem. 56, 599 (1952).
[15]J. F. Emery, Oak Ridge National Laboratory Report No. ORNL-3889, 1965 (unpublished).
[16]H. Müller, Umschau Wiss. Tech. 17, 534 (1968).
[17]H. Buser and P. Graf, Angew. Chem. 66, 277 (1954).
[18]J. Pauly, Compt. Rend. 240, 2415 (1955).
[19]T. B. Novey, Atomic Energy Commission Report No. CC-1631, 1944 (unpublished).
[20]L. V. Groshev, A. M. Demidov, V. I. Pelekhov, L. L. Sokolovskii, G. A. Bartholomew, A. Doveika, K. M. Eastwood, and S. Monaro, Nucl. Data 5A, 243 (1969).
[21]C-H. Hsiung, H-C. Hsiung, and A. A. Gordus, J. Chem. Phys. 34, 535 (1961).
[22]The penetration of a moving particle into matter is best discussed in terms of the mass of material traversed (e.g., $\mu g/cm^2$)—that is, the distance multiplied by the density of the medium—rather than in terms of the distance itself (e.g., cm). In the present experiments, this convention is an obvious necessity.
[23]This can be readily seen by noting that in helium the observed recoil fraction (Fig. 3 or 5) does not decrease from the value in vacuum until there is a certain amount of helium in the gap, which implies that essentially all of the recoils have a correspondingly significant component of motion in a direction normal to the plane of the gold surface (i.e., there are few recoils emitted at low angles with the surface).
[24]J. H. Jeans, *An Introduction to the Kinetic Theory of Gases* (Cambridge U. P., Cambridge, England, 1940), pp. 53 and 54.
[25]M. Knudsen, *The Kinetic Theory of Gases: Some Modern Aspects*, 3rd ed. (Methuen, London, 1950), pp. 26–29.
[26]N. F. Ramsey, *Molecular Beams* (Oxford U. P., London, 1956), pp. 45, 46.
[27]W. Feller, *An Introduction to Probability Theory and Its Applications* (Wiley, New York, 1950), Vol. I, Sec. XIV. 8.
[28]G. Friedlander, J. W. Kennedy, and J. M. Miller, *Nuclear and Radiochemistry*, 2nd ed. (Wiley, New York, 1964), pp. 118–120.
[29]D. J. Hughes, *Pile Neutron Research* (Addison-Wesley, Cambridge, Mass., 1953), pp. 25–27.
[30]S. Dushman, in *Scientific Foundations of Vacuum Technique*, 2nd ed., edited by J. M. Lafferty (Wiley, New York, 1962), pp. 25–32.

PHYSICAL REVIEW B VOLUME 4, NUMBER 9 1 NOVEMBER 1971

Cubic-Site EPR Spectra of Eu^{2+} and Gd^{3+} in MgO Single Crystals*

M. M. Abraham, L. A. Boatner,† Y. Chen, J. L. Kolopus, and R. W. Reynolds†
Solid State Division, Oak Ridge National Laboratory, Oak Ridge, Tennessee 37830
(Received 14 June 1971)

The electron-paramagnetic-resonance spectra of Gd^{3+} and Eu^{2+} in cubic sites of MgO single crystals have been observed. Spin-Hamiltonian parameters for these ions have been determined as a function of temperature. The observed variation of the fourth-order spin-Hamiltonian parameter c vs lattice constant for the alkaline-earth oxides implies that in MgO overlap and covalency must be considered in determining the ground-state splitting of these ions.

INTRODUCTION

Although numerous electron-paramagnetic-resonance (EPR) investigations of iron-group impurities in magnesium oxide single crystals have been performed, until the recent observation[1] by EPR of Yb^{3+} in MgO, the only rare-earth resonance spectrum reported for this host was that of Er^{3+}.[2] Detailed studies of several rare-earth ions have been carried out, however, using the isomorphic (NaCl-type structure) hosts CaO, SrO, and BaO. Of these studies, the experiments[3–13] dealing with the impurity ions Eu^{2+} and Gd^{3+} ($4f^7$ configuration, $^8S_{7/2}$ ground state) are considered to be particularly significant, since they emphasize the inability of current models to account for crystal-field effects on the $^8S_{7/2}$ ground state. The cubic spectrum of Eu^{2+} in the oxides was especially interesting in that the fourth-order spin-Hamiltonian parameter was observed to vary from a positive quantity for Eu^{2+} in BaO, to approximately zero in SrO, to a negative quantity in CaO. A variation of this nature is clearly beyond the predictions of a simple crystal-field model. Additionally, the sign

of the fourth-order spin-Hamiltonian parameter for Gd^{3+} in the three oxides, where the Gd^{3+} impurity is coordinated with six nearest neighbors, was determined to be the same as that for Gd^{3+} when coordinated with eight nearest neighbors. This result is again unexpected on the basis of any rudimentary model for the crystal-field interaction.

Incorporating Eu^{2+} and Gd^{3+} in single-crystal MgO would make it possible to study the effects of a reduced lattice size on the signs and magnitudes of the spin-Hamiltonian parameters, and to compare temperature variations of the ground-state splittings with the other alkaline-earth oxides and with fluorite-structure hosts. Additionally, MgO is ideally suited for investigations of the effects of both uniaxial stress and pressure on S-state splittings. For these reasons numerous attempts have been made during the past several years to observe EPR spectra of either Eu^{2+} or Gd^{3+} in MgO single crystals. All previous attempts have been unsuccessful and no $^8S_{7/2}$ spectra of any symmetry type have been reported for this host.

The purposes of this paper are to report the initial observation of cubic-site EPR spectra for Eu^{2+} and Gd^{3+} in MgO single crystals, to present the spin-Hamiltonian constants which have been determined as a function of temperature, and to examine the implications of these results as they relate to the general question of cubic-field splittings of S states arising from f^7 configurations.

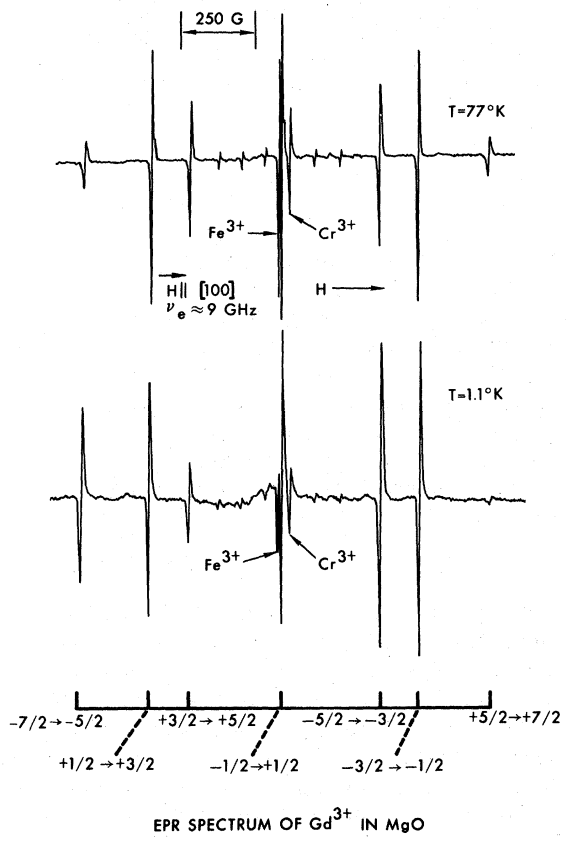

FIG. 1. EPR spectrum of Gd^{3+} in MgO at 77 and 1.1 K for $\vec{H} \parallel [100]$. The change in relative intensity of the lines with decreasing temperature indicates that c is negative.

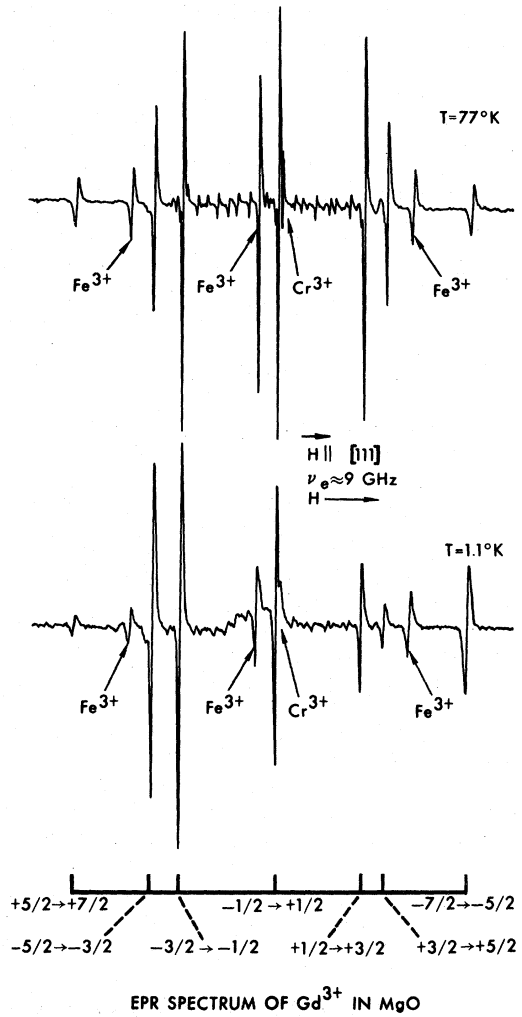

FIG. 2. EPR spectrum of Gd^{3+} in MgO at 77 and 1.1 K for $\vec{H} \parallel [111]$. The change in relative intensity of the lines with decreasing temperature indicates that c is negative.

EXPERIMENT

The Eu^{2+}- and Gd^{3+}-doped single crystals used in this investigation were grown by the arc-fusion technique.[14] The starting material consisted of high-purity MgO powder[15] to which the appropriate rare-earth oxide had been added. EPR spectra were observed at a frequency of approximately 9 GHz using both a conventional homodyne spectrometer and a superheterodyne system for mea-

TABLE I. Spin-Hamiltonian parameters for Gd^{3+} and Eu^{2+} in MgO.

Temp. (K)	g	c (10^{-4} cm^{-1})	d (10^{-4} cm^{-1})
	Gd^{3+}		
Room	1.9920±0.0005	−134.5±0.2	+8.5±0.1
77	1.9920±0.0005	−139.8±0.2	+8.8±0.1
4.2	1.9920±0.0005	−140.0±0.2	+8.8±0.1
	Eu^{2+}		
77	1.9894±0.0005	−291.8±0.4	+14.7±0.2
4.2	1.9894±0.0005	−292.6±0.4	+14.6±0.2

surements at 4.2 K or below.

In MgO single crystals doped with Gd^{3+}, a cubic-symmetry EPR spectrum was observed at room and lower temperatures. Figures 1 and 2 show the MgO: Gd^{3+} spectra obtained at 77 and 1.1 K with the magnetic field applied parallel to a fourfold symmetry axis and a threefold symmetry axis, respectively. The seven $\Delta M_s = \pm 1$ transitions are identified at the bottom of the figures. Spectra due to Cr^{3+}, Fe^{3+}, and Mn^{2+} are also present. The changes in relative intensities with temperature apparent in this figure fix the signs of the transitions and determine the sign of the fourth-order spin-Hamiltonian parameter as negative. The angular dependence of the Gd^{3+} spectrum is shown in Fig. 3 and illustrates the cubic-symmetry variation. It is important to notice in Fig. 3 that although the ordering of the $\Delta M_s = \pm 1$ transitions with $\vec{H} \| [100]$ is identical to that observed for Gd^{3+} in the fluorite-structure hosts, the ordering when the magnetic field is applied parallel to a [111] direction is not.[16] For $\vec{H} \| [111]$, the $-\frac{1}{2} \rightarrow -\frac{3}{2}$ and $-\frac{3}{2} \rightarrow -\frac{5}{2}$ lines on the low-field side of the spectrum and the $+\frac{3}{2} \rightarrow +\frac{1}{2}$ and $+\frac{5}{2} \rightarrow +\frac{3}{2}$ lines on the high-field side are interchanged from their ordering in the eightfold-coordinated hosts. This interchange occurs because the ratio of the crystal-field parameters B_6/B_4 is larger for Gd^{3+} in the sixfold-coordinated oxides than in the fluorite-structure hosts.

The cubic-site spectrum of Eu^{2+} was not seen in "as-grown" MgO crystals. After γ irradiation at either 77 or 295 K, cubic Eu^{2+} resonance transitions were observed due to the conversion of some europium to the divalent state. The resonance spectrum could not be observed at room temperature, but could be seen at 77 K and at lower temperatures. Axial Eu^{2+} spectra were not observed. Linewidths of individual Eu^{2+} hyperfine components were very small (less than 1 G wide) and the 12 hyperfine components due to the two isotopes ^{151}Eu and ^{153}Eu were clearly resolved.

The cubic-symmetry spectra of Eu^{2+} and Gd^{3+} were fitted to the spin Hamiltonian[17]

$$\mathcal{H} = g\mu_B \vec{H} \cdot \vec{S} + B_4[O_4^0 + 5O_4^4] + B_6[O_6^0 - 21O_6^4] \quad (1)$$

by means of a computer program which performed an exact diagonalization of the matrix corresponding to the $S = \frac{7}{2}$ ground state. For the analysis of hyperfine structure, Eq. (1) was appropriately modified by addition of the term $A\vec{I} \cdot \vec{S}$. The spin-Hamiltonian parameters determined for Eu^{2+} and Gd^{3+} are shown in Table I, where the usual notation $c = 240B_4$ and $d = 5040B_6$ is employed. Additionally, the following hyperfine parameters were determined (in 10^{-4} cm^{-1}): for Eu^{2+} (at 77 K), $^{151}A = -31.63 \pm 0.10$ and $^{153}A = -13.95 \pm 0.10$; and for Gd^{3+} (at 296 K), $^{155}A = 3.85 \pm 0.05$ and $^{157}A = 5.06 \pm 0.05$.

DISCUSSION

Previous investigations of the effects of lattice size, temperature, pressure, and uniaxial stress on the ground-state splittings of $4f^7$-configuration ions have established that competing interactions are responsible for the observed splittings, and that these interactions include terms containing quadratic and higher powers of the crystal-field potential. Although a great deal of attention has been given to studies of these ions in the cubic fluorite-structure hosts, the information provided by the investigations using alkaline-earth-oxide hosts is believed to be more significant for two principal rea-

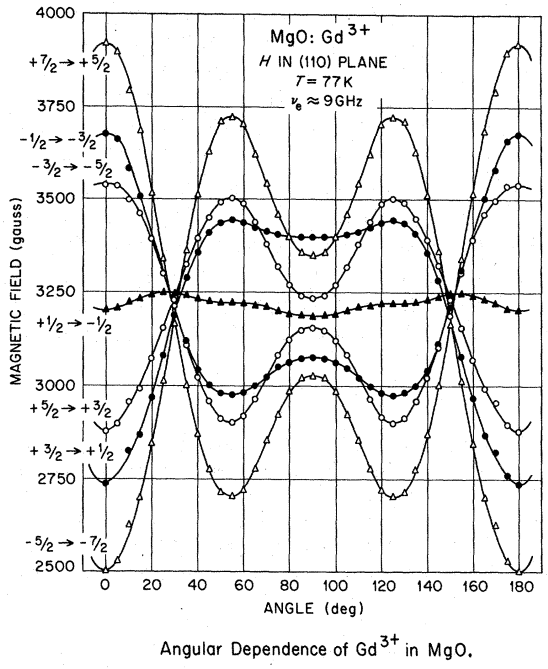

FIG. 3. Angular dependence of the MgO: Gd^{3+} EPR spectrum for $\vec{H}$ in the (110) plane. The angle 0° corresponds to the [001] axis, 54.74° corresponds to the $[\bar{1}11]$ axis, and 90° to the $[\bar{1}10]$ axis.

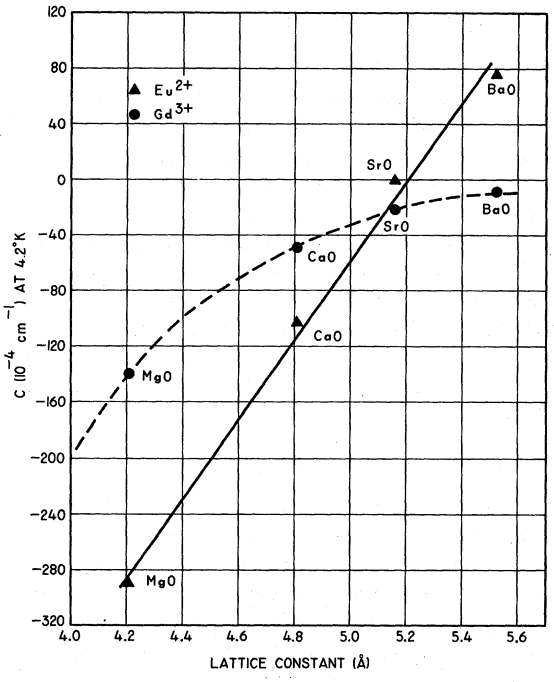

FIG. 4. Dependence of the Eu^{2+} and Gd^{3+} fourth-order spin-Hamiltonian parameter c on lattice constant for the alkaline-earth oxides.

sons: First, the ground-state splittings of Eu^{2+} in the oxides provide a reference point at which competing interactions produce a null effect. Second, with the addition of the data presented here, a more definite trend in the variation of S-state splitting with lattice size can be established. (This is possible since the MgO:Eu^{2+} and MgO:Gd^{3+} data greatly extend the range of host-lattice sizes for the oxide series relative to that for the alkaline-earth fluorides.) Combining the present data with those obtained for BaO, SrO, and CaO, it is apparent that the fourth-order spin-Hamiltonian parameter c obtained for Eu^{2+} varies linearly with lattice constant a_0, while that of Gd^{3+} does not.[8] The Eu^{2+} fourth-order parameters are fitted by the equation $c = 284.3a_0 - 1480$, where a_0 is expressed in angstroms and c in 10^{-4} cm^{-1}. The linear correlation coefficient of 0.996 for this fit shows that there is only a 0.4% probability that four random points would fit a straight line to this accuracy or better. A plot of c vs a_0 for europium and gadolinium is shown in Fig. 4. The slope of the c-vs-a_0 curve for Gd^{3+} is seen to increase rapidly with decreasing a_0 at the CaO data point where the ionic radii of Gd^{3+} and Ca^{2+} are approximately equal. Near the MgO data point, the slope determined for Gd^{3+} approaches that found for Eu^{2+}.

In view of the disparity in ionic sizes between Mg^{2+} and the Eu^{2+} and Gd^{3+} impurity ions, considerable overlap is expected between the paramagnetic impurity and the coordinating ions. (Indeed, it is remarkable that these ions can be incorporated substitutionally in MgO. The presence of cubic-symmetry sites with minimal lattice strains, as evidenced by the narrow lines, is even more unexpected.) The similarity in the slopes at the MgO data point implies that overlap and covalency are more important in determining the splitting in MgO than they are in the more inflated lattices. The larger splitting found for Eu^{2+} relative to Gd^{3+} in MgO supports this implication since the ionic radius of Eu^{2+} is larger than that of Gd^{3+}. Although overlap and covalency should continue to be more important for Eu^{2+} than Gd^{3+} in the hosts with larger cation sizes, other mechanisms appear to dominate in these hosts. Similar dependences of the fourth-order parameter c on lattice size for Eu^{2+} and Gd^{3+} in the alkaline-earth fluorides are suggested from the available data but are less dramatic due to the restricted range of lattice-constant variation.

Considering the systematics of lattice size and ionic radius and their relation to the observed splittings, we suggest that overlap and covalency should be given a more detailed treatment than they have previously received in attempts to calculate $^8S_{7/2}$ ground-state splittings.

---

*Research sponsored by the U.S. Atomic Energy Commission under contract with Union Carbide Corporation.

†Advanced Technology Center, Inc., Dallas, Tex.

[1]R. W. Reynolds, M. M. Abraham, L. A. Boatner, and Y. Chen, Bull. Am. Phys. Soc. 16, 360 (1971).

[2]D. Descamps and Y. Merle D'Aubigne, Phys. Letters 8, 5 (1964).

[3]J. Overmeyer and R. J. Gambino, Phys. Letters 9, 108 (1964).

[4]A. J. Shuskus, J. Chem. Phys. 41, 1885 (1964).

[5]J. L. Kolopus, thesis (University of Missouri, Columbia, Mo., 1965) (unpublished).

[6]B. A. Calhoun and J. Overmeyer, J. Appl. Phys. 35, 989 (1964).

[7]A. J. Shuskus, Phys. Rev. 127, 2022 (1962).

[8]W. Low and R. S. Rubins, in *Proceedings of the First International Conference on Paramagnetic Resonance*, edited by W. Low (Academic, New York, 1963), Vol. 1, p. 79; Phys. Letters 1, 316 (1962).

[9]K. E. Mann and L. V. Holroyd, Phys. Status Solidi 28, K27 (1968).

[10]L. A. Boatner and M. M. Abraham (unpublished).

[11]W. Low and J. T. Suss, Phys. Letters 11, 115 (1964).

[12]J. L. Kolopus, L. V. Holroyd, and K. E. Mann, Phys. Status Solidi 9, K95 (1965).

[13]M. M. Abraham, L. A. Boatner, E. J. Lee, and R. A. Weeks, in Proceedings of the Sixth Rare-Earth

Research Conference, Gatlinburg, Tenn., 1967 (unpublished).
[14]C. T. Butler, B. J. Sturm, and R. B. Quincy, Jr., J. Cryst. Growth 8, 197 (1971); M. M. Abraham, C. T. Butler, and Y. Chen, J. Chem. Phys. (to be published).
[15]Kanto Chemical Company, Tokyo, Japan.
[16]See, for example, M. M. Abraham, L. A. Boatner, C. B. Finch, E. J. Lee, and R. A. Weeks, J. Phys. Chem. Solids 28, 81 (1967).
[17]K. R. Lea, M. J. M. Leask, and W. P. Wolf, J. Phys. Chem. Solids 23, 1381 (1962).

PHYSICAL REVIEW B VOLUME 4, NUMBER 9 1 NOVEMBER 1971

Track-Effect Theory of Scintillation Efficiency

Myron Luntz
Department of Physics, State University of New York at Fredonia, Fredonia, New York 14063
(Received 7 June 1971)

A theoretical account is presented of the pulse-height characteristics of NaI(Tl) scintillation counters subjected to energetic heavy-ion bombardment ($Z \geq 5$, $E/A = 1$–10 MeV/nucleon) at room temperature. The falling off of scintillation efficiency dL/dE with decreasing energy and the charge dependence at fixed energy are simultaneously accounted for by introducing the concept of a cylinder of high energy-deposit density surrounding the particle track. Inside the cylinder competitive events, favored by high ionization density, are assumed to dominate those which produce the characteristic luminescence emission. Agreement with experiment is best for high-Z particles. Cylinder radii vary over the range $110 \lesssim R_c(Z, v) \lesssim 390$ Å. Estimates of the fraction of the total energy loss available for efficient light production yield the values $0.20 \lesssim F_0(Z, v) \lesssim 0.50$, while the critical value of energy-deposit density defining the high-density cylinder is approximated to be 5.32×10^7 erg/cm^3. Also, a brief discussion is presented regarding interpretation of the heavy-ion pulse-height characteristics of pure alkali halides at low temperature, and those of anthracene and NE 102 plastic scintillators, in terms of the track-effect theory.

I. INTRODUCTION

The purpose of this paper is to provide a theoretical account of the response of activated alkali iodide scintillation counters to room-temperature bombardment by energetic heavy ions and, in so doing, to present a theory applicable to a fairly wide range of scintillating crystals. Treated explicitly are the data of Newman and Steigert[1] for NaI(Tl) corresponding to bombardment with B^{10}, C^{12}, N^{14}, O^{16}, F^{19}, and Ne^{20} ions of incident energies ranging from approximately 1 to 10 MeV/nucleon. The curves displaying relative pulse heights, shown in Fig. 1, are linear at the higher energies, and become distinctly nonlinear as E decreases. The direction of curvature implies a systematic falling off of scintillation efficiency dL/dE with the slowing down of a particle. Also apparent is a dependence of pulse height on particle identity, such that the lighter the ion, the greater is the total light output for the same total energy loss.

Detailed explanations have been offered to account for these features.[2–4] However, the treatments of Refs. 2 and 4 include explicit assumptions regarding luminescence mechanisms which have been demonstrated to be invalid or, at best, highly dubious. Also, several processes which are operative during the penetration of a highly ionizing particle—processes which are likely to have a profound effect on the luminescent response—are disregarded. The treatment of Ref. 3 suffers from difficulties of a somewhat different nature which, along with the above points, are discussed in the paper. Further examination of the problem would appear to be in order.

The present formulation incorporates the so-called "track-effect" profile of energy deposit about the path of a penetrating ion.[5] An imaginary cylinder surrounding the particle track is employed to partition the crystal into regions of high and low energy-deposit density. Associated with each region is a corresponding contribution to the total scintillation efficiency. Upon consideration of events favored by high ionization density, e.g., electron-hole recombination and radiation-damage and lattice-heating effects, and upon consideration of the competitive role of such events with respect to luminescence, the assumption is made that dL/dE receives a negligible contribution from within the high-density region. In contrast, the response to energy deposited outside the high-density cylinder is assumed to be linear. Thus, the total light production efficiency of a particle of atomic number Z and velocity v is determined solely by the energy deposit at distances from the track which exceed